

Sine Approximation for Direct Digital Frequency Synthesizers and Function Generators

Milan Stork

Applied Electronics and Telecommunications, Faculty of Electrical Engineering/RICE
University of West Bohemia, CZ
Univerzitni 8, 30614 Plzen
CZECH REPUBLIC
stork@kae.zcu.cz

Abstract: - There are several compression methods for phase to amplitude converter for sine function. In this paper, the linear and parabolic approximation of equi-section division utilizing the symmetry property and amplitude approximation of a sinusoidal waveform for direct digital frequency synthesizer (DDS) and also for other waveform applications, e.g. function generators and telecommunication devices is proposed. The sinusoidal phase from 0 to $\pi/2$ is divided into different numbers of equi-sections. The linear and parabolic approximations are compared. The simulation results show spectral properties of booth approach. The presented sine approximation is usable for FPGA implementation.

Key-Words: Direct digital synthesis, frequency spectrum, frequency synthesizers, linear approximation, parabolic approximation, phase to amplitude converter, simulation.

1 Introduction

Direct digital frequency synthesis is increasingly welcomed in modern communication systems and precise electronic systems, due to their significant advantages over phase-locked loop (PLL) based synthesizers. Fast frequency switching, excellent frequency resolution, continuous-phase switching and low phase noise are important features easily obtainable in direct digital synthesizers is a well-known technique for the generation of a sinusoidal waveform reconfigurably [1]. DDS techniques have lots of advantages over analog approaches beyond flexibility, including excellent frequency resolution, fast response time, fast frequency switching, and low phase noise.

The DDS architecture, is shown in Fig. 1. The system has two inputs: a clock frequency f_{clk} and a frequency control word (FCW). The phase accumulator accumulates the value of the FCW in every clock cycle, periodically overflowing. Its ramp output is considered as a phase in the interval $\langle 0, 2\pi \rangle$, while the phase-to-sinusoid amplitude converter provides a digital amplitude value of the sinusoidal waveform of that phase. The output frequency of DDS is given by

$$f_o = f_{clk} \frac{FCW}{2^N} \quad [\text{Hz}] \quad (1)$$

The sequences of digital amplitude values pass through a digital-to-analog converter (DAC) and

usually to low-pass filter (LPF) to generate a sinusoidal signal [2].

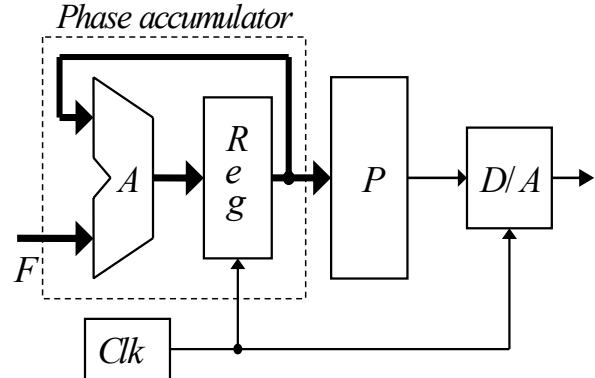


Fig. 1. The DFS architecture block diagram.
 F - frequency control word, Clk - clock generator,
 Reg – register, P – phase-to-sine amplitude converter, D/A – digital/analog converter.

There are a wide variety of methods for phase to sine-amplitude conversion [3, 4, 5], from full-memory to full-hardware approaches. The methods can be placed into three categories.

a) Based on ROM lookup tables (LUT), containing amplitude samples of the complete, half, or quarter period of sinusoid, and addressed by the digital phase, which is generated by the phase accumulator [1, 2].

b) Full computational methods, trying to compute the sine amplitude samples from the digital phase, which is generated by the phase accumulator. Sine computation by using Taylor series [1] and CORDIC algorithm [6] are two examples of this category.

c) Initial guess correction methods, in which an initial guess for the sine function is generated by digital hardware and then is corrected by small ROM lookup table, containing the difference between the initial guess and the accurate value for the sine amplitude. If the initial guess is properly provided, in each memory location just small correcting data will be stored instead of the whole sine amplitude. It is obvious that the closer the approximation is to ideal sine function, the more memory saving there will be.

There are several ROM compression methods, such as the quarter-wave symmetry method [7], the sine amplitude approximation, eg.

Sine-Phase Difference Algorithm [2].

Modified Sunderland Architecture [4].

Nicholas' Architecture [2].

Taylor Series Approximation [5].

The another possibility is ROM-less DDS with Sin-weighted DAC.

With the quarter-wave symmetry method, the ROM only needs to store one-quarter (the phase from 0 to $\pi/2$) of the sine wave sequences [8 - 15]. The two most significant bits (MSBs) of the phase value determine to which quadrant an angle belongs, while the residual $M-2$ bits are used to address a one-quadrant sine LUT.

In this paper, the linear and parabolic approximation of equi-section division is proposed as a ROM compression method which utilizes the property of the quarter-wave symmetry method as well as sine amplitude approximation. The length of period in all simulations is 4096 and sine amplitude is ± 4095 ($2^{13}-1$).

The MSE (mean square error) is calculated according (2)

$$MSE = \sum_{i=1}^N (y_i - \sin_i(.))^2 \quad (2)$$

2 Linear and Parabolic Approximation

The sinusoidal phase from 0 to $\pi/2$ is divided into s equi-sections, where s is the parameter by which to decide the number of equi-sections. The coefficients for linear and polynomial approximations are derived by least squares sense method.

The example of linear approximation (for 4

sections) is shown in Fig. 2, and example of parabolic approximation (also for 4 sections) is displayed in Fig. 3. The error of approximation is also shown. The sinusoidal phase from 0 to $\pi/2$ is divided into equi-sections.

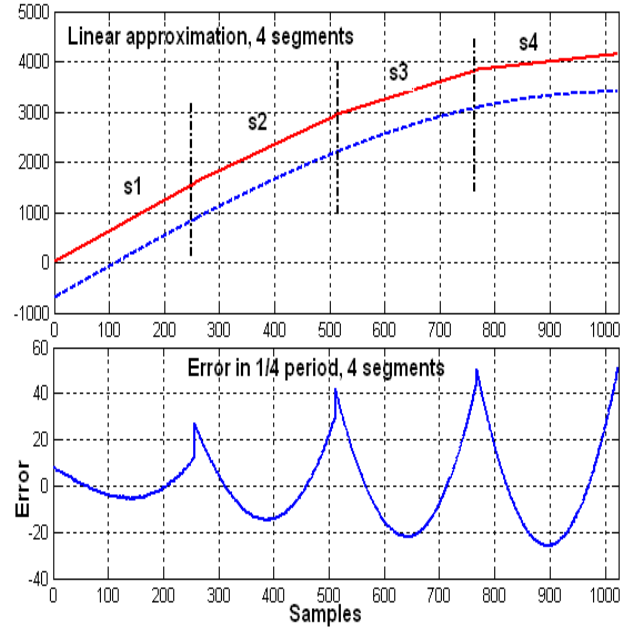


Fig. 2. Example of linear approximation quarter of sine (top) and approximation error (bottom).

Approximation – solid line (red), sine – dash line (blue), shifted down.
(4 segments s1, s2, s3, s4 are used).

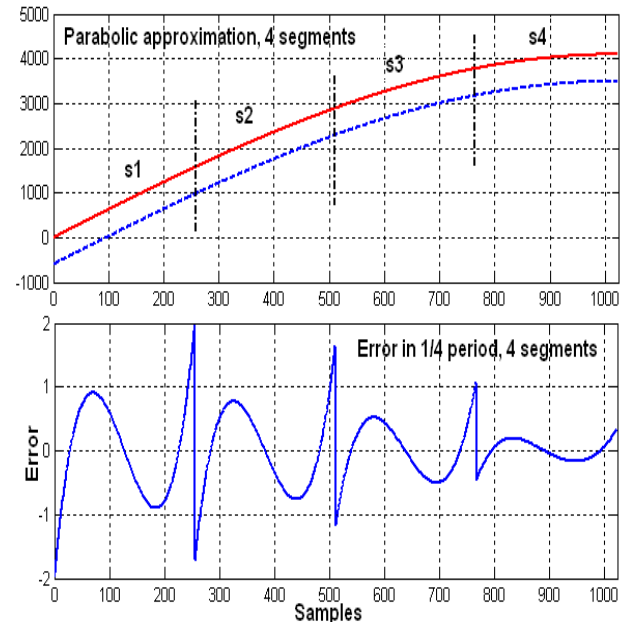


Fig. 3. Example of parabolic approximation quarter of sine (top) and approximation error (bottom).

Approximation – solid line (red), sine – dash line (blue), shifted down.
(4 segments s1, s2, s3, s4 are used).

Equation (3) below gives the slopes and shift for linear approximation (example for 4 segments) as

$$4095 \cdot \sin\left(2\pi \frac{x}{4096}\right) \approx y = \begin{cases} 6.138x + 8; & 0 \leq x < 256 \\ 5.205x + 261; & 256 \leq x < 512 \\ 3.48x + 1155; & 512 \leq x < 768 \\ 1.225x + 2892; & 768 \leq x < 1024 \end{cases} \quad (3)$$

Result is shown in Fig. 2.

Equation (4) shows the equations for parabolic approximation (example for 4 segments)

$$4095 \cdot \sin\left(2\pi \frac{x}{4096}\right) \approx y = \begin{cases} -0.0009x^2 + 6.37x - 1.98; & 0 \leq x < 256 \\ -0.0027x^2 + 7.25x - 116; & 256 \leq x < 512 \\ -0.0040x^2 + 8.59x - 456; & 512 \leq x < 768 \\ -0.0047x^2 + 9.66x - 860; & 768 \leq x < 1024 \end{cases} \quad (4)$$

Result is shown in Fig. 3.

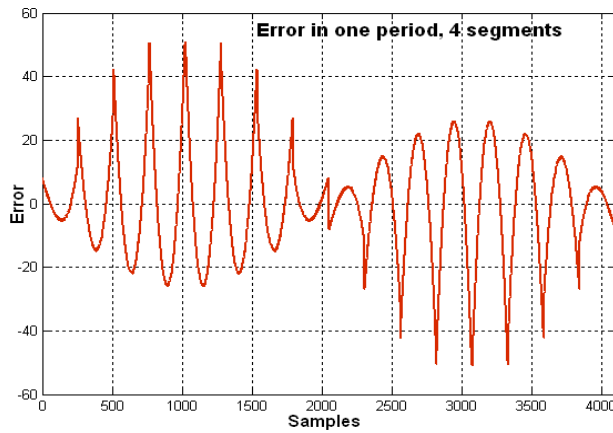


Fig. 4. Example of error calculated for 1 period for linear approximation and 4 segments.

3 Linear Approximation for 4, 8, 16, 32 and 64 segments

In this chapter the simulation results for segment number of 4, 8, 16, 32 and 64 are shown. The MSE (Mean square error) errors and spectral properties were calculated and are presented in Tab. 1. The example of error for 1 period is shown in Fig. 4, spectral properties in Fig. 5 - 9. From Tab. 1 can be seen, that almost optimal is 32 segments (quarter of period, 0 to $\pi/2$ is divided to 32 equidistant segments).

Tab. 1. Linear approximations with different number of segments.

No. of segment	MSE	dBc
4	1.13e+6	-47.9
8	7.10e+4	-60.1
16	4.76e+3	-72.1
32	612.2	-106.0
64	378.7	-104.9

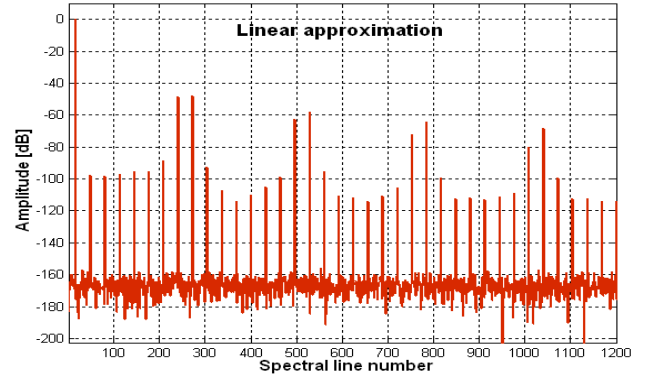


Fig. 5. The output frequency spectrum, calculated for 4 segments and linear approximation.

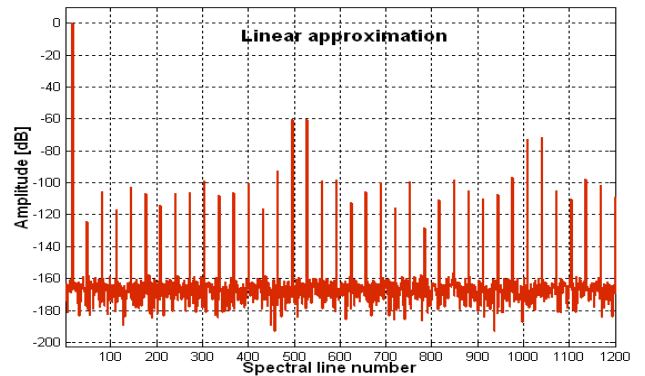


Fig. 6. The output frequency spectrum, calculated for 8 segments and linear approximation.

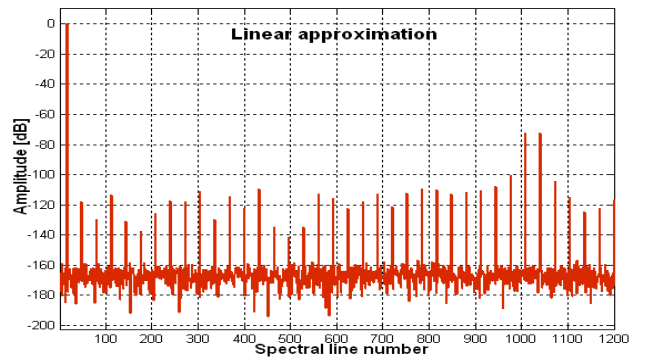


Fig. 7. The output frequency spectrum, calculated for 16 segments and linear approximation.

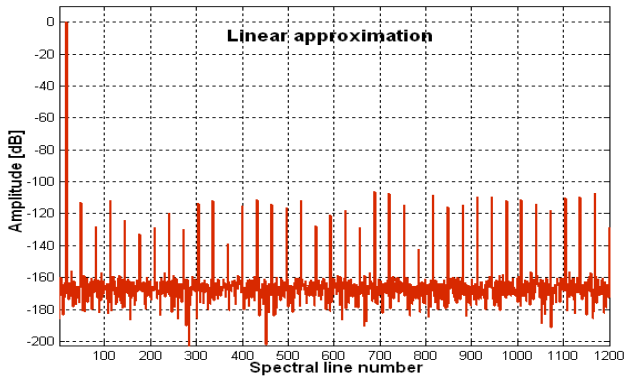


Fig. 8. The output frequency spectrum, calculated for 32 segments and linear approximation.

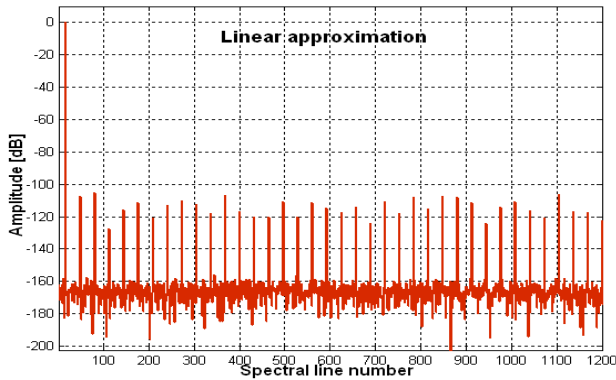


Fig. 9. The output frequency spectrum, calculated for 32 segments and linear approximation.

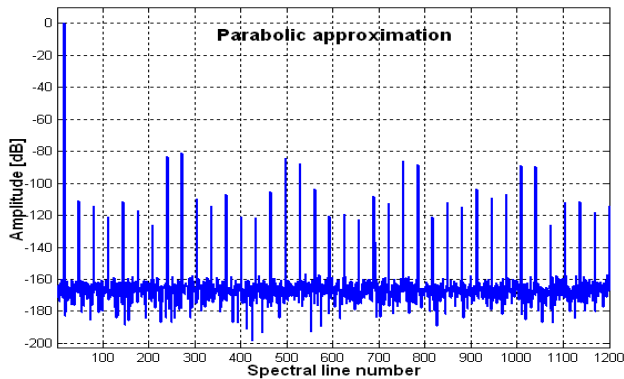


Fig. 10. The output frequency spectrum, calculated for 4 segments and parabolic approximation.

4 Parabolic Approximation for 4, 8 and 16 segments

In this chapter the simulation results for segment number of 4, 8, and 16 are shown. The MSE (Mean square error) errors and spectral properties were calculated and are presented in Tab. 2. The spectral properties are also displayed in Fig. 10 - 12. From Tab. 2., can be seen, that 16 segments of parabolic approximation is similar to 64 segments of linear approximation.

Tab. 2. Parabolic approximations with different number of segments.

No. of segment	MSE	dBc
4	1.5307e+003	-81.2
8	374.6	-95.8
16	356.9	-102.9

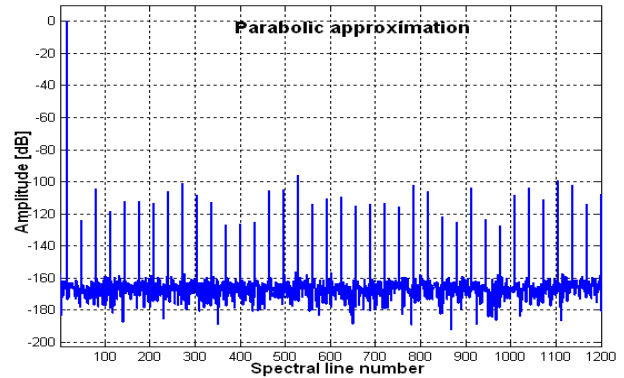


Fig. 11. The output frequency spectrum, calculated for 8 segments and parabolic approximation.

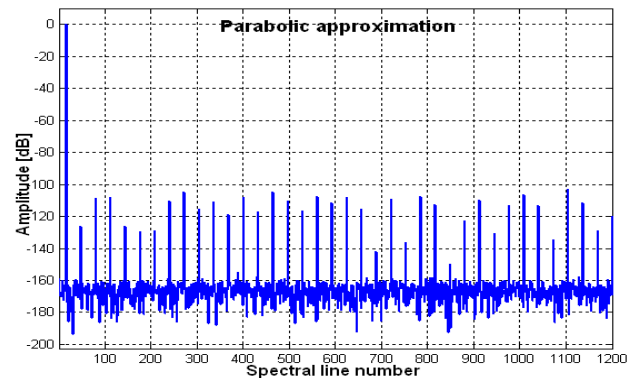


Fig. 12. The output frequency spectrum, calculated for 16 segments and parabolic approximation.

5 Conclusion

Ultrahigh speed direct digital synthesizers will play important roles in next generation radar and communication systems. Recent developments in radar systems require frequency synthesis with low power consumption, high output frequency, fine frequency resolution, fast channel switching and versatile modulation capabilities. Linear frequency modulation or chirp modulation is widely used in radars to achieve high range resolution, while pulsed phase modulation can provide anti-jamming capability. With fine frequency resolution, fast channel switching and versatile modulation capabilities, the DDS provides frequency synthesis and direct modulation capabilities that cannot be

easily implemented by other synthesizer tools such as analog-based phase-locked loop synthesizers.

In this paper, the linear and parabolic approximation of equi-section division utilizing the quarter-wave symmetry method and sine amplitude approximation was described, calculated and simulated. The sinusoidal phase from 0 to $\pi/2$ was divided into different numbers of equi-sections, in linear approximation from 4 to 64, in parabolic approximation from 4 to 16 sections. The calculated values were rounded to integer numbers and frequency spectrum of simulated sine function was presented. The proposed compression method can be applied for DDS, software defined radio (SDR) systems, spread spectrum frequency hopping systems, and a variety of signaling applications.

Acknowledgment

This research was supported by the European Regional Development Fund and Ministry of Education, Youth and Sports of the Czech Republic under project No. CZ.1.05/2.1.00/03.0094: Regional Innovation Centre for Electrical Engineering (RICE)

References:

- [1] J. Vankka and K. Halonen, *Direct Digital Synthesizers*, Kluwer Academic Publishers, ISBN 0-7923-7366-9, 2001
- [2] H. T. Nicholas, H. Samuelli, and B. Kim, The Optimization of Direct Digital Frequency Synthesizer in the Presence of Finite Word Length Effects Performance, *Proc. 42nd Annu. Frequency Contr. Symposium*, June 1988, pp. 357-363.
- [3] P. W. Ruben, E. F. Heimbecher, II, and D. L. Dilley, Reduced Size Phase-to-Amplitude Converter in a Numerically Controlled Oscillator, *U. S. Patent 4855946*, Aug. 8, 1989.
- [4] D. A. Sunderland, R. A. Strauch, S. S. Wharfield, H. T. Peterson, and C. R. Cole, CMOS/SOS Frequency Synthesizer LSI Circuit for Spread Spectrum Communications, *IEEE J. of Solid State Circuits*, Vol. SC-19, 1984, pp. 497-505.
- [5] L. A. Weaver, and R. J. Kerr, High Resolution Phase To Sine Amplitude Conversion, *U. S. Patent 4905177*, 1990.
- [6] J. E. Volder, The CORDIC Trigonometric Computing Technique, *IRE Trans. On Electron. Comput.*, EC-8:330-334, 1959.
- [7] D. De Caro, N. Petra, and A. G. M. Strollo, Reducing lookup-table size in direct digital frequency synthesizers using optimized multipartite table method, *IEEE Trans. Circuits Syst. I, Reg. Papers*, vol. 55, no. 7, 2008, pp. 2116-2127.
- [8] J. M. P. Langlois, and D. Al-Khalili, Phase to sinusoid amplitude conversion techniques for direct digital frequency synthesis, *IEE Proc.-Circuits Devices Syst.*, vol. 151, no. 6, 2004, pp. 519-528.
- [9] J.M.P. Langlois and D. Al-Khalili, Hardware optimized direct digital frequency synthesizer architecture with 60 dBc spectral purity, *IEEE International Symposium on Circuits and Systems (ISCAS 2002)*, May 2002.
- [10] D. De Caro, and A. G. M. Strollo, High-performance direct digital frequency synthesizers using piecewise-polynomial approximation, *IEEE Trans. Circuits Syst. I, Reg. Papers*, vol. 52, no. 2, 2005, pp. 324-337.
- [11] L. S. J. Chimakurthy, M. Ghosh, F. F. Dai, and R.C. Jaeger, A novel DDS using nonlinear ROM addressing with improved compression ratio and quantization noise, *IEEE Trans. Ultrason., Ferroelectr., Freq. Control*, vol. 53, no. 2, 2006, pp. 274-283.
- [12] A. M. Sodagar, and G. Roientan Lahiji, Mapping from phase to sine-amplitude in direct digital frequency synthesizers using parabolic approximation, *IEEE Trans. Circuits Syst. II, Analog Digit. Signal Process.*, vol. 47, no. 12, 2000, pp. 1452-1457.
- [13] A. M. Sodagar, and G. Roientan Lahiji, A pipelined ROM-less architecture for sine-output direct digital frequency synthesizers using the second-order parabolic approximation, *IEEE Trans. Circuits Syst. II, Analog Digit. Signal Process.*, vol. 48, no. 9, 2001, pp. 850-857.
- [14] S. Hermann, and R. Klette, A Comparative Study on 2D Curvature Estimators, *International Conference on Computing: Theory and Applications*, 2007, pp. 584-589.
- [15] K.I. Palomaki and J. Niitylahti, Direct digital frequency synthesizer architecture based on Chebyshev approximation, *Proceedings of the 34th Asilomar Conference on Signals, Systems and Computers*, 2000, pp. 1639-1643.
- [16] B. G. Goldberg, *Digital Techniques in Frequency Synthesis*, New York: McGraw-Hill, 1996.
- [17] V.F. Kroupa, V. Cizek, J. Stursa, and H. Svandova, Spurious signals in direct digital frequency synthesizers due to the phase truncation, *IEEE Transactions on Ultrasonics, Ferroelectrics, and Frequency Control*, vol. 47, no. 5, September 2000, pp. 1166-1172.

Appendix: Spurious modulation of DDS

The DDS output waves at the digital to analog convertors (DAC), with normalized output frequencies close to the ratio of small integers, exhibit either a "quasi-amplitude" modulation in some instances (see Fig. 13) and a "quasi-superposition" (see Fig. 14) of the desired high frequency wave on a low frequency signal, as mentioned in [16, 17], e.g. for expansion:

$$FCW/2^n = 253/1024$$

$$\frac{X}{Y} = \frac{253}{1024} = \frac{1}{b_1 + \frac{1}{b_2 + \frac{1}{b_3}}} = \frac{1}{4 + \frac{1}{21 + \frac{1}{12}}} \quad (A1)$$

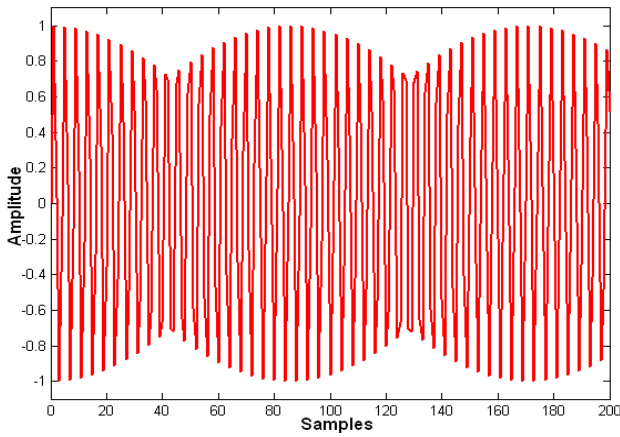


Fig. 13. Example of quasi-amplitude modulation for DDS, $FCW/2^n = 253/1024$

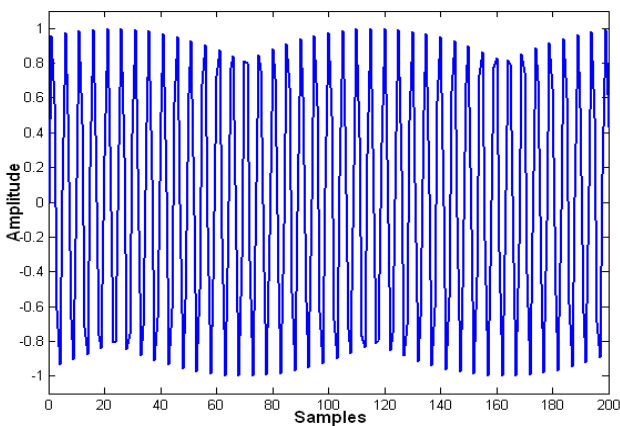


Fig. 14. Example of quasi-superposition for DDS, $FCW/2^n = 207/1024$

The continued fraction expansion is given by

$$\frac{X}{Y} = \frac{1}{B_0 B_1} - \frac{1}{B_1 B_2} + \frac{1}{B_2 B_3} \dots \frac{(-1)^n}{B_n B_{n+1}} \quad (A2)$$

where

$$\begin{aligned} B_0 &= 1 \\ B_1 &= b_1 \\ B_2 &= b_2 B_1 + B_0 \\ B_3 &= b_3 B_2 + B_1 \\ &\dots \\ B_n &= b_n B_{n-1} + B_{n-2} \end{aligned} \quad (A3)$$

In previous example ($X/Y = 253/1024$) $b_1=4$, $b_2=21$, $b_3=12$ (function "rat" in MATLAB returns the continued fraction representation, b_1 , b_2 , b_3) and according (A3):

$$B_1=4; B_2=21*4+1=85; B_3=12*85+4=1024$$

and therefore:

$$\begin{aligned} \frac{X}{Y} &= \frac{253}{1024} = \\ &= \frac{1}{3} - \frac{1}{4*85} + \frac{1}{85*1024} = 0.2470703125 \end{aligned}$$

For second example $X/Y = 207/1024$, the $b_1=54$, $b_2=-19$, $b_3=5$, $b_4=2$ and expansion is:

$$\begin{aligned} \frac{X}{Y} &= \frac{207}{1024} = \frac{1}{5} - \frac{1}{5*(-94)} + \frac{1}{(-94)*(-465)} \\ &\quad - \frac{1}{(-465)*(-1024)} = 0.2021484375 \end{aligned}$$

The output sine wave of DDS can be simplified to:

$$\begin{aligned} s(m) &= \sin\left(2\pi m \frac{X}{Y}\right) \approx \\ &\approx \sin\left[2\pi m \left(\frac{1}{B_1} \pm \frac{1}{B_1 B_2}\right)\right] \end{aligned} \quad (A4)$$

The trigonometric expansion gives:

$$\begin{aligned} s(m) &= \sin\left(2\pi m \frac{1}{B_1}\right) \cos\left(2\pi m \frac{1}{B_1 B_2}\right) \\ &\quad \pm \cos\left(2\pi m \frac{1}{B_1}\right) \sin\left(2\pi m \frac{1}{B_1 B_2}\right) \quad (A5) \\ &= s_1(m) \pm s_2(m) \end{aligned}$$

From expansion can be seen that low frequency component cause "quasi-amplitude" modulation or "quasi-superposition" for some FCW numbers.